Ecological Modelling 263 (2013) 223–232

Contents lists available at SciVerse ScienceDirect

Ecological Modelling

journal homepage: www.elsevier.com/locate/ecolmodel

Tracking *Acropora* fragmentation and population structure through thermal-stress events

L. Roth[a,*], E.M. Muller[a,b], R. van Woesik[a]

[a] Department of Biological Sciences, Florida Institute of Technology, 150 West University Boulevard, Melbourne, FL 32901, USA
[b] Mote Marine Laboratory, 1600 Ken Thompson Parkway, Sarasota, FL 34236, USA

ARTICLE INFO

Article history:
Received 6 December 2012
Received in revised form 3 May 2013
Accepted 7 May 2013
Available online 14 June 2013

Keywords:
Corals
Temperature
Modeling
Size frequency distributions
Bayesian
Climate

ABSTRACT

Fragmentation of reef corals spreads the risk of encountering unfavorable environments. High rates of fragmentation, however, may give the false impression of expanding, diversifying populations when instead the populations are simply cloning. We developed a discrete model that tracked the contribution of fragments to the coral populations by monitoring two thermally sensitive corals, branching coral *Acropora palmata* and corymbose *Acropora* colonies before, during, and after thermal-stress events at Haulover Bay, in the US Virgin Islands (Caribbean) and at Aka Jima in southern Japan (Pacific), respectively. We hypothesized that fragmentation rates would increase following disturbance years for both *Acropora* taxa. Using a Bayesian approach we tested the fit of the models with the observed data. Fragmentation was more frequent for *A. palmata* in the Caribbean than for corymbose *Acropora* in southern Japan. The highest frequency of fragmentation for *A. palmata* occurred during and soon after thermal stress, increasing the population density but shifting the size-frequency distribution toward small colonies. Fragmentation of corymbose *Acropora* in southern Japan was generally low and relatively constant throughout the study, except during thermal stress, which resulted in the loss of the smallest and largest colonies, effectively narrowing the size-frequency distribution.

1. Introduction

Fragmentation is the separation of a single genotype into two or more individuals; it is the predominant mode of reproduction of many branching reef corals, especially those within the family Acroporidae (Highsmith, 1982; Heyward and Collins, 1985; Lirman, 2000). In some localities corals may rely solely on fragmentation for persistence (Baums et al., 2006), by spreading the risk of encountering unfavorable local environments (Jackson, 1977; Highsmith, 1982). Fragmentation of colonies may result from direct physical breakage by waves, boat anchors, groundings, and snorkeler interactions.Fragmentation may be an indirect consequence of predation, sedimentation, bleaching, or infectious diseases, which causes partial colony mortality and subsequent fragmentation. At times, corals can regenerate lesions caused by partial colony mortality and fuse back with the original colony (Meesters and Bak, 1993). However, whether or not regeneration and fusion occurs depends on lesion size and species-specific thresholds (Bak and Steward-van Es, 1980).

Fragmentation also has its costs, especially in rapidly changing environments (van Woesik and Jordan-Garza, 2011; Graham and van Woesik, 2013). For example, survival of fragments is positively associated with fragment size, and small fragments tend to have a high rate of mortality (Highsmith et al., 1980). Frequent fragmentation may also reduce tolerance to thermal stress and disease (Muller et al., 2008). As a result, what may appear to be a healthy population may turn out to be the remains of a scattered, single genotype (Baums et al., 2005, 2006). Therefore, high densities of coral colonies with low-genetic diversity might give the false impression of a large, resistant population. Low-genetic diversity could also lead to suppressed recovery after disturbances and local and regional extinction (Ellstrand and Elam, 1993; Worm et al., 2006). Understanding the state of genetic diversity within populations and how that diversity changes over time are essential for implementing the most effective conservation strategies (Baums et al., 2006).

The highest rates of fragmentation typically occur during stress events, such as during large storms or at times of high water temperatures. Anomalously high water temperatures may lead to coral bleaching, when corals lose their symbiotic algae (Brown, 1997). During coral bleaching events, the rates of partial colony mortality also typically increase, because corals cannot survive without their algal symbionts for prolonged periods (Hoegh-Guldberg, 1999). Often the upper portions of branching colonies, which are directly exposed to irradiance, bleach more readily than the undersides of colonies (Lesser, 1996). The upper portions of branching

* Corresponding author. Tel.: +1 321 735 4898.
E-mail address: lynnette.roth@gmail.com (L. Roth).

0304-3800/$ – see front matter © 2013 Elsevier B.V. All rights reserved.
http://dx.doi.org/10.1016/j.ecolmodel.2013.05.002

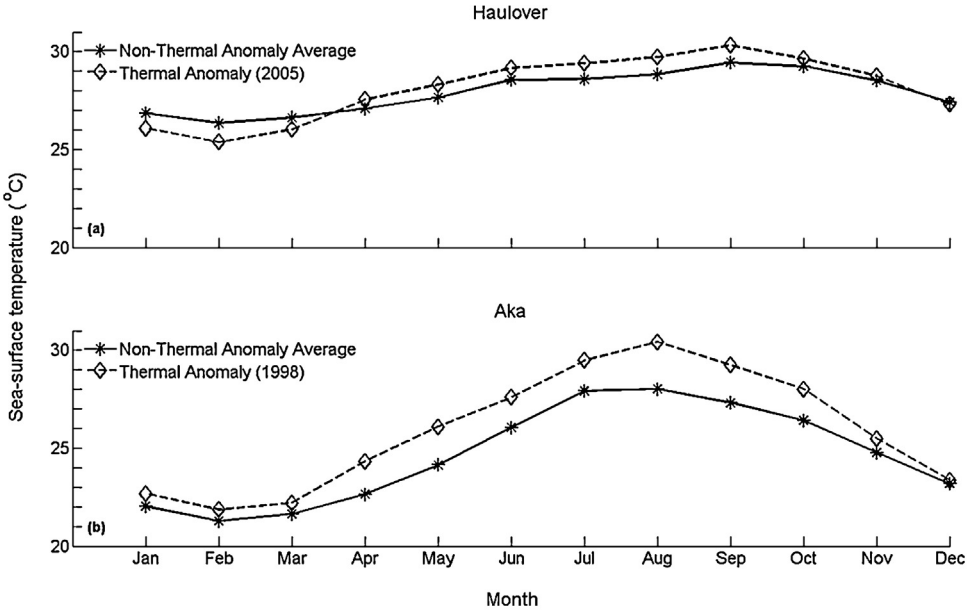

Fig. 1. (a and b) The monthly temperature data for both: (a) Haulover Bay, US Virgin Islands, and (b) Aka Jima, Japan, throughout each study period. The thermal anomaly occurred in 1998 at Aka Jima and in 2005 at Haulover Bay.

colonies are also subjected to more partial mortality than the undersides of branching colonies. Regardless of the location of partial mortality, the loss of live tissue provides new substrate for bio-eroding organisms, which decreases the integrity of the skeleton and increases the probability of colony fragmentation (Glynn, 1997). Likewise, an outbreak of coral disease frequently occurs during or soon after anomalous temperature events (Muller et al., 2008; Rogers and Muller, 2012), leading to partial colony mortality and increased rates of colony fragmentation (Glynn, 1997).

To date there has been little effort to model the change of single genotypes, or genets, into two or more individuals, or ramets (Heyward and Collins, 1985). Most models use Lefkovitch transition matrices (Lefkovitch, 1965; Hughes, 1984; Done, 1987; Lirman, 2000) that do not distinguish genets from ramets. Indeed, the dynamics of clonal life histories are not accurately captured in Lefkovitch matrices (Orive, 1995), and the negative repercussions of colony fragmentation have been largely ignored. For example, colony fragmentation is most often interpreted as positive recovery of the populations being modeled, because the fragmentation process adds new colonies to the population (Hughes, 1984; Done, 1987). However, new fragments are not 'new' genotypes, and high densities of coral colonies of low-genetic diversity may increase a population's susceptibility to disturbances, especially when those genotypes are intolerant to stress.

In this study, we developed a model that tracked both genets and ramets through time. The model was developed and tested using *Acropora palmata*, a species once common throughout the Caribbean, and corymbose *Acropora*, common on reefs in the Indian and Pacific Oceans. The *A. palmata* colonies were monitored on the reefs of the United States Virgin Islands (USVI) and the corymbose *Acropora* colonies were monitored on the reefs of Aka Jima in southern Japan. During our study, thermal anomalies occurred within each region; in the USVI in 2005 (Eakin et al., 2010) and in Aka Jima, Japan, in 1998 (Roth et al., 2010; Fig. 1). We hypothesized that thermal-stress events would increase the fragmentation rates of the *Acropora* colonies. To test this hypothesis we monitored the fragmentation rates of individual colonies through time. Our objectives were to: (1) quantify the fragmentation rates before, during, and after thermal-stress events for two different *Acropora* corals (i.e., corymbose *Acropora* in southern Japan and the branching coral *A. palmata* in the Caribbean), (2) determine changes in the *Acropora* size-frequency distributions at each locality through time, and (3) model the effects of *Acropora* fragmentation on the generation rates of ramets to accurately predict changes in the densities of ramets and genets through time.

2. Methods

2.1. Fragmentation rates and changes in size-frequency distributions

We were interested in comparing the fragmentation rates of common *Acropora* colonies in both the Caribbean and in the Indo-Pacific through thermal-stress events. From 2003 to 2010, branching *A. palmata* colonies were monitored at 0–2 m in Haulover Bay, St. John, USVI (Rogers and Muller, 2012), and from 1996 to 2000, corymbose *Acropora* were tracked at 0–1 m at Kushibaru, Aka Jima, southern Japan (Roth et al., 2010). Fragmentation rates were determined by calculating the percentage of new-living fragments compared with the total number of colonies present during each yearly transition.

The longest diameter (assuming an ellipse) of each *Acropora* colony was measured either in situ (St. John) or from photographs (Aka Jima). Each colony was tracked through time to determine colony growth, partial mortality, fragmentation, and mortality rates for each yearly transition (Tables 1–4). *A. palmata* was the only species measured at St. John, whereas corymbose *Acropora*, measured at Aka Jima, was an amalgamation of morphologically similar species composed mainly of *A. nasuta* (Roth et al., 2010). Each *Acropora* colony from Haulover Bay was placed into one of twelve size-class bins, consisting of 10 cm increments (0.1–10, 10.1–20, . . ., >110 cm), whereas each colony from Aka Jima was placed into one of seven size-classes (i.e., 0.1–10, 10.1–20, . . ., >60 cm). This separation allowed for an adequate number of colonies within each size class to discern a distribution and to thereby track that distribution through time. Using a Bayesian goodness-of-fit approach

Table 1
Fragmentation rates for: (a) averaged non-thermal years, and (b) the 2005 thermal anomaly year in Haulover Bay, US Virgin Islands. The matrix shows the rate that the row size-class number fragmented into the column size-class number.

Size class	1	2	3	4	5	6	7	8	9	10	11	12
(*a*) *Haulover averaged non-thermal years*												
1	0.03	0.02	0	0	0	0	0	0	0	0	0	0
2	0	0	0	0	0	0	0	0	0	0	0	0
3	0.03	0	0	0	0	0	0	0	0	0	0	0
4	0.24	0.07	0	0	0	0	0	0	0	0	0	0
5	0.24	0.07	0	0	0	0	0	0	0	0	0	0
6	0.06	0.13	0.11	0	0	0	0	0	0	0	0	0
7	0.67	0.33	0.33	0.61	0	0	0	0	0	0	0	0
8	0.33	0.11	0.22	0	0	0	0	0	0	0	0	0
9	0.31	0.11	0	0.11	0	0	0	0	0	0	0	0
10	0.05	0.25	0.30	0.10	0	0	0	0	0	0	0	0.11
11	0	0	0	0	0	0	0	0	0	0	0	0
12	0.33	0.07	0.29	0.11	0.29	0	0	0.11	0	0.29	0	0
(*b*) *Haulover thermal anomaly year* ($\Delta 2005$)												
1	0.07	0	0	0	0	0	0	0	0	0	0	0
2	0	0	0	0	0	0	0	0	0	0	0	0
3	0.60	0	0.10	0	0	0	0	0	0	0	0	0
4	0.25	0	0	0	0	0	0	0	0	0	0	0
5	0.67	0.11	0	0	0	0	0	0	0	0	0	0
6	0	0.50	0	0.25	0	0	0	0	0	0	0	0
7	0.67	0.33	0	0	1.00	0.33	0	0	0	0	0	0
8	0	0	0	0	0	0	0	0	0	0	0	0
9	0.17	0.17	0	0	0.17	0.17	0.17	0	0	0	0	0
10	0	0.25	0	0	0	0	0	0	0	0	0	0
11	4.00	2.00	1.00	2.00	0	1.00	0	0	0	0	0	0
12	1.20	0.40	0	0	0	0	0	0	0	0	0	0.20

(Betancourt, 2010), we compared the observed size-frequency distributions with the normal (Gaussian), chi-square, and log-normal distributions.

2.2. The genet-ramet model

Our primary objective was to develop a discrete-time model that tracked individual genets and ramets through time. Rogers and Muller (2012) showed that 94% of the population of *A. palmata* at Haulover Bay was genotypically distinct. However, for our purposes each initial colony was assumed to be genetically distinct at t_0. The initial population abundance matrix, P, was a $1 \times n \times S$ matrix, where n was the number of size classes, and S was the total number of genetically distinct colonies (genets) in the population at the initial-time step (t_0). For example, if the initial population abundance was three colonies, two of which were in the first size class and one of which was in the second size class, the P matrix could be defined as:

$$P = \begin{matrix} & & & & & & [1 & 0 & 0 & \cdots & 0] \\ & & & & & \iddots & & & & \iddots & \\ & & & & [1 & 0 & 0 & \cdots & 0] & & \\ & & & \iddots & & & & \iddots & & & \\ & & [0 & 1 & 0 & \cdots & 0] & & & & \end{matrix} \quad (1)$$

Similar densities of sexual recruits were added to both localities to focus on the sensitivities of the fragmentation process rather than on new inputs by recruits. Each recruited colony was added to the smallest size class (x_1) as a new layer in the matrix, increas-

Table 2
Fragmentation rates for: (a) averaged non-thermal years, and (b) the 1998 thermal anomaly year in Aka Jima, Japan. The matrix shows the rate that the row size-class number fragmented into the column size-class number.

Size class	1	2	3	4	5	6	7
(*a*) *Aka averaged non-thermal years*							
1	0	0	0	0	0	0	0
2	0.04	0	0	0	0	0	0
3	0	0.04	0	0	0	0	0
4	0	0	0.03	0	0	0	0
5	0	0.07	0.15	0	0	0	0
6	0	0.11	0.22	0	0	0	0
7	0	0	0	0.11	0	0	0
(*b*) *Aka thermal anomaly year* ($\Delta 1998$)							
1	0	0	0	0	0	0	0
2	0	0	0	0	0	0	0
3	0	0	0	0	0	0	0
4	0	0	0	0	0	0	0
5	0	0	0	0	0	0	0
6	0	0	0	0.50	0	0	0
7	0	0	0	0	0	0	0

Table 3
Adjusted Lefkovitch transition matrices for: (a) averaged non-thermal years, and (b) the 2005 thermal anomaly year in Haulover Bay, US Virgin Islands. The upper, right-hand triangle gives rates of growth, whereas the lower, left-hand triangle gives rates for partial mortality that have been adjusted to account for fragmentation. The bottom row gives rates of mortality for each size class.

Size class	1	2	3	4	5	6	7	8	9	10	11	12
(*a*) *Haulover averaged non-thermal years*												
1	0.51	0.11	0.03	0	0	0	0	0	0	0	0	0
2	0.11	0.26	0.10	0.20	0.03	0.02	0	0	0	0	0	0
3	0.05	0.08	0.24	0.18	0.14	0.07	0	0	0	0	0	0
4	0.29	0.14	0.09	0.26	0.20	0.12	0.03	0.02	0	0	0	0
5	0.33	0.14	0.07	0	0.16	0.20	0.22	0.12	0	0	0	0
6	0.11	0.20	0.11	0	0.12	0.19	0.17	0.07	0.22	0	0.11	0
7	0.67	0.33	0.50	0.61	0	0.17	0	0	0.56	0	0	0.11
8	0.33	0.11	0.22	0	0	0.17	0	0	0.44	0.11	0.11	0.17
9	0.42	0.11	0	0.11	0	0	0	0	0.25	0.56	0.08	0
10	0.05	0.25	0.30	0.10	0.11	0.05	0	0	0	0.05	0.05	0.86
11	0	0	0	0	0	0	0	0	0	0.33	0	0.33
12	0.33	0.07	0.29	0.18	0.36	0	0.11	0.11	0	0.40	0.07	0.58
Mortality	0.40	0.29	0.27	0.14	0.07	0	0	0	0	0	0	0
(*b*) *Haulover thermal anomaly year* (*Δ2005*)												
1	0.64	0	0.07	0	0	0	0	0	0	0	0	0
2	0.08	0.42	0.08	0	0	0	0	0	0	0	0	0
3	0.80	0.10	0.20	0.20	0.10	0	0	0	0	0	0	0
4	0.33	0.17	0.17	0.42	0.08	0	0.08	0	0	0	0	0
5	0.78	0.22	0.11	0	0.11	0.11	0.11	0	0	0	0	0
6	0.25	0.50	0	0.25	0.25	0.25	0	0.25	0	0	0	0
7	0.67	0.33	0	0	1.00	0.33	0	0.33	0.67	0	0	0
8	0	0	0.25	0	0	0	0	0.25	0	0.50	0	0
9	0.17	0.17	0	0	0.33	0.17	0.17	0	0.33	0.33	0.17	0
10	0	0.50	0	0	0	0	0	0	0	0.50	0	0.25
11	4.00	2.00	1.00	2.00	0	2.00	0	0	0	0	0	0
12	1.20	0.40	0	0	0	0	0	0	0	0.20	0.20	0.80
Mortality	0.36	0.42	0.30	0	0.33	0	0	0	0	0	0	0

ing S (number of genets). We modeled recruitment as a Poisson distribution, defined by the following equation:

$$y = f(x \mid \mu) = \frac{\mu^x e^{-\mu}}{x!} \tag{2}$$

where μ was the sample mean number of recruits observed in the field. For each yearly iteration, the number of recruits was randomly selected from the data-fitted Poisson distribution (Roth et al., 2010), and added to the abundance matrix P. Post-settlement mortality was estimated in Aka Jima (Roth et al., 2010), and was used in both locations because post-settlement mortality was not quantified in Haulover Bay.

Table 4
Adjusted Lefkovitch transition matrices for: (a) averaged non-thermal years, and (b) the 1998 thermal anomaly year in Aka Jima, Japan. The upper, right-hand triangle gives rates of growth, whereas the lower, left-hand triangle gives rates for partial mortality that have been adjusted to account for fragmentation. The bottom row gives rates of mortality for each size class.

Size class	1	2	3	4	5	6	7
(*a*) *Aka averaged non-thermal years*							
1	0.50	0.23	0	0	0	0	0
2	0.11	0.50	0.19	0.02	0	0	0
3	0.04	0.26	0.62	0.06	0	0	0
4	0	0	0.17	0.63	0.17	0	0
5	0	0.07	0.22	0.08	0.62	0.15	0
6	0.11	0.11	0.22	0	0.11	0.17	0.17
7	0	0	0	0.11	0.11	0.28	0.61
Mortality	0.28	0.21	0.06	0.06	0.08	0.44	0
(*b*) *Aka thermal anomaly year* (*Δ1998*)							
1	0.25	0.58	0	0	0	0	0
2	0	0.42	0.33	0	0	0	0
3	0	0.27	0.33	0.27	0	0	0
4	0	0	0	0.83	0.17	0	0
5	0	0.20	0	0	0.40	0.20	0
6	0	0	0	1.00	0.50	0	0
7	0	0	0	0	0	0	1.00
Mortality	0.17	0.25	0.13	0	0.20	0	0

The matrix P_{t_0} was then multiplied by the Lefkovitch transition matrix (M), which was derived from field data collected at each respective locality (Rogers and Muller, 2012; Roth et al., 2010; Tables 3 and 4). Their product created a new abundance matrix, P_{t_1}, for the following time step. In order to derive M, we first defined an initial Lefkovitch matrix, L, as:

$$L = \begin{bmatrix} l_{1,1} & l_{1,2} & l_{1,3} & \dots & l_{1,n} \\ l_{2,1} & l_{2,2} & l_{2,3} & \dots & l_{2,n} \\ l_{3,1} & l_{3,2} & l_{3,3} & \dots & l_{3,n} \\ \vdots & \vdots & \vdots & \ddots & \vdots \\ l_{n,1} & l_{n,2} & l_{n,3} & \dots & l_{n,n} \end{bmatrix} \tag{3}$$

where, reading the matrix from row to column, the upper-right triangle of the matrix represents growth (e.g. $l_{1,2}$ represents growth from size class 1 to 2), the diagonal represents the proportion of colonies that do not change size class (e.g. $l_{1,1}$), and the lower-left triangle represents partial mortality (e.g. $l_{3,1}$ represents a colony originating in size class 3 shrinking or splitting into a colony of size class 1; Fig. 2). While fragmentation is a form of partial mortality, it can be found, theoretically, in any of the above transitions. If a colony split and created colonies that had time to grow into larger size classes, before the next measurement was taken, fragmentation would be added to the upper-right triangle. If a colony split but created colonies that stayed in the same size classes, fragmentation rates would be added to the diagonal of the matrix. In most cases, however, fragmentation creates colonies in the smallest size class, adding fragmentation rates to the lower-left triangle of the matrix (Fig. 2). The mortality rate for each row (i.e., size class) is derived by summing each row and subtracting from 1. In a standard Lefkovitch matrix, all three of these rates (growth, partial mortality, and mortality) sum to one. For our model, we adjusted these rates to include rates of fragmentation calculated in the field. For example, for a transition from size class 4 to size class 3 (because

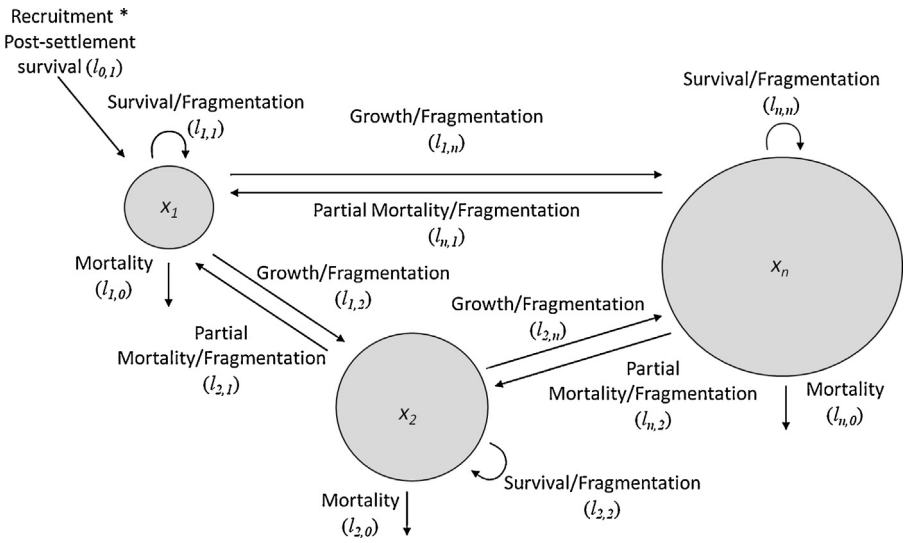

Fig. 2. Schematic representation of three representative coral colony size classes and the major processes within the genet-ramet model. Variables in parentheses represent the position of the measured process within the Lefkovitch matrix.
This figure has been adapted from Roth et al. (2010).

of partial mortality or fragmentation), the density of size-class 3 is divided by the original density in the larger size class 4. These calculations thereby account for all additions to the population through fragmentation while still taking into account the other calculated rates. If fragmentation rates were high enough to exceed mortality rates, then that particular row could sum to >1, adding ramets to the system.

To provision for a carrying capacity, we defined the proportion of space available for growth as K:

$$K = f(x_1, x_2, \ldots, x_n) = \frac{1 - \left[(C - Ac) + \sum_{i=1}^{n} c_i x_i\right]}{(1 - C)} \quad (4)$$

where colony size class was defined by x_i, C was the total proportional cover of all the corals present in each quadrat, and Ac was the total proportional cover of all study coral colonies (*A. palmata* or corymbose *Acropora*) at the initial time step, in each quadrat. The constant c_i was determined by:

$$c_i = \frac{\overline{a_{x_i}}}{T}, i = 1, \ldots, n \quad (5)$$

where $\overline{a_{x_i}}$ was the average area occupied by a colony in the size class x_i and T was the total sample space (i.e., quadrat or reef surface area). The abundance of colonies in each size class is then multiplied by the corresponding c_i to estimate the density of *Acropora* in each size class at each time step, allowing colony density to vary through time. All the size-class densities were summed to give a total proportion of area covered by the study species at each time step. The carrying capacity was then divided by (1-C) to normalize the density to the initial conditions, or to normalize the density to the existing carrying capacity. The revised Lefkovitch matrix, which takes into account fragmentation, can be expressed in the following form:

$$M = \begin{bmatrix} l_{1,1} & l_{1,2} & l_{1,3} & \cdots & l_{1,n} \\ l_{2,1} & l_{2,2} & l_{2,3} & \cdots & l_{2,n} \\ l_{3,1} & l_{3,2} & l_{3,3} & \cdots & l_{3,n} \\ \vdots & \vdots & \vdots & \ddots & \vdots \\ l_{n,1} & l_{n,2} & l_{n,3} & \cdots & l_{n,n} \end{bmatrix} * \begin{bmatrix} 1 & K & K & \cdots & K \\ 1 & 1 & K & \cdots & K \\ 1 & 1 & 1 & \cdots & K \\ \vdots & \vdots & \vdots & \ddots & K \\ 1 & 1 & 1 & \cdots & 1 \end{bmatrix} \quad (6)$$

where the upper-right triangle of the first matrix represents growth, which is adjusted by K in the second matrix to account for carrying capacity, and the lower-left triangle of the first matrix represents partial mortality. A new 3-dimensional matrix (P_{t_1}) was formed by multiplying each layer of P_{t_0} independently with M, which remains constant through all time steps. For each time step, the total population was calculated by summing all colonies present within all layers of the resulting matrix. The number of genets was given by summing the number of layers (S) within the resulting matrix P_{t_1}, whereas the number of ramets was calculated by finding the difference between the total population and the number of genets.

2.3. Simulations

We conducted a series of simulations of population trajectories using equations 1–4 for *A. palmata* from Haulover Bay and for corymbose *Acropora* data from Aka Jima. As a Lefkovitch matrix gives data for the transition between years, these transitional data are indicated by delta (Δ), which represents a change from the listed year to the following year (i.e. Δ2003 represents the transition from 2003 to 2004). The model was run for each yearly transition for which that data were available (Haulover: 2003–2007; Aka Jima: 1996–2000), giving a total of 4 simulations for each location. These simulations provided a projection of the size-frequency distribution of each population through time. We also conducted a disturbance simulation, which combined two different Lefkovitch matrices that used all data from each location. The first Lefkovitch matrix was an average of every data matrix, excluding data for the thermal-stress year (Δ2005 for Haulover Bay and Δ1998 for Aka Jima). The averaged matrix, representing all non-thermal-stress years, was used for every time step, except for when simulating the thermal-stress year, for which we used Δ2005 and Δ1998 data to mimic the thermal-stress events that occurred in the field.

Using a Bayesian approach (Betancourt, 2010), we compared the size-frequency distributions of the final year of the observed field data (i.e., 2010 at Haulover Bay and 2000 at Aka Jima) with the same corresponding year of each simulation (i.e., for Δ2003, simulation data from year 7 was used). With this approach, the observed and simulated distributions were compared with two different Bayesian distribution models: (1) where the distributions

Table 5
Results from the log-normal curve fit comparing frequency of *A. palmata* (Haulover Bay, US Virgin Islands) and corymbose *Acropora* colonies (Aka Jima, Japan) by size class (Fig. 4). μ: mean; σ: variance.

Site	Year	μ	σ	R^2
Haulover	2003	1.248	0.426	0.941
	2004	1.383	1.313	0.829
	2005	53.200	18.650	0.906
	2006	0.000	2.392	0.957
	2007	1.331	1.153	0.855
	2010	0.957	0.606	0.718
Aka	1996	0.930	0.664	0.977
	1997	0.976	0.560	0.990
	1998	1.038	0.708	0.842
	1999	1.039	0.493	0.850
	2000	1.013	0.571	0.901

were drawn from the same, over-lapping distribution ($\pi = 1$), and (2) where the distributions were drawn from non-overlapping distributions ($\pi = 0$), assuming a uniform, non-informative prior distribution. For these models, π represents a mixture coefficient that describes the relative contribution of each model (1 and 2) to the final distribution. The over-lapping distribution model best described the simulated and observed size-frequencies when $\pi > 0.5$, whereas, the non-overlapping distribution model best described the simulated and observed size-frequencies when $\pi < 0.5$. All models were run with MATLAB® 2009 (and are available upon request).

3. Results

Fragmentation rates observed in the field were much higher for *A. palmata* colonies at Haulover Bay than for corymbose *Acropora* colonies at Aka Jima (Tables 1 and 2; Fig. 3). At Haulover Bay, the highest number of fragments formed during the thermal anomaly in 2005, when the number of ramets far exceeded the number of genets (Figs. 3 and 4). Additionally, the size-frequency distribution of *A. palmata* shifted toward small colonies during, and soon after, the 2005-thermal-stress event (Fig. 5). By contrast, at Aka Jima there was a relatively low but consistent fragmentation rate through time (Fig. 3). During the 1998-thermal-stress event in Aka Jima, fragmentation rates did not increase (Fig. 3), although there was a reduction of both genets and ramets (Figs. 3 and 4; Table 2). The population of colonies in Aka Jima showed a loss in the smallest and largest colonies following the thermal-stress event, effectively narrowing the distribution, although when compared with the *A. palmata* distributions the corymbose *Acropora* distributions remained relatively consistent through time (Fig. 5). For both locations, a log-normal distribution was consistently the best-fit distribution for the size-frequency data (Fig. 5; Table 5).

The Bayesian analysis that examined goodness of fit, indicated that at Haulover Bay the modeled size-frequency distributions were not similar to the observed size-frequency distributions (i.e., drawn from non-overlapping distributions), at least when we used the data matrices for Δ2003 and Δ2004 to parameterize the models (Fig. 6). The Δ2005 simulation (i.e., the thermal anomaly transition) yielded the highest π value, indicating it was the closest fit model to the observed field data (Fig. 6). The highest generation of ramets of *A. palmata* in the USVI occurred when projecting the Δ2004 matrix through time (Fig. 4). Notably the Δ2004 transition occurred in a non-thermal-stress year, when the large colonies (>110 cm) either had split or had partially died. The consequence of fragmentation of these large colonies, although there were few large colonies, had major repercussions on subsequent trajectories (Fig. 4; Tables 1 and 3). By contrast, all years that were modeled at Aka Jima, showed a good fit with the observed size-frequency distributions, independent of the year for which the transition matrices were constructed (Fig. 7).

4. Discussion

The results of our study suggest that the fragmentation rate and therefore the size-frequency distributions of the branching coral *A. palmata* in the USVI were more sensitive to thermal-stress events than corymbose *Acropora* populations in Aka Jima. The thermal-stress event in 2005, at Haulover Bay, St. John, shifted the already log-normal distribution toward even smaller colonies. However, by the end of the study, five years later, there was a shift toward large colonies, as small colonies grew and transitioned into larger size classes. By contrast, corymbose *Acropora* lost both large and small colonies at Aka Jima, Japan, but there was less change in the overall shape of the log-normal distribution through time.

Still, the resulting size-frequency distribution of a particular *Acropora* population will ultimately depend of the intensity of the disturbance. As noted by Roth et al. (2010), the coral colonies on the reefs of Aka Jima in 1998 experienced a +1.8 °C temperature anomaly, narrowing the size-frequency distribution of corymbose *Acropora*. By contrast, the coral colonies on reefs surrounding Sesoko Island in southern Japan, in the same year (1998), were subjected to a more extreme +3 °C temperature anomaly. Only *Acropora* colonies <9 cm in diameter survived the extreme thermal event at Sesoko Island, shifting the size-frequency distribution to a highly positively-skewed distribution (Loya et al., 2001).

The present study also suggests that while Indo-Pacific corymbose *Acropora* spp. are susceptible to bleaching-induced mortality (Loya et al., 2001; Stimson et al., 2002), they rarely undergo partial mortality and survive. By contrast, *A. palmata* in the Caribbean tended to fragment during the thermal-stress event and survive. Therefore, the 2005-thermal-stress event increased the ramet density of *A. palmata*, but tended to select out thermally intolerant genotypes of corymbose *Acropora*. As a consequence, the ramet to genet ratio did not vary much through time on Aka Jima, whereas *A. palmata* showed the potential for rapid population growth (Fig. 4), caused primarily by an increase in the number of ramets, while maintaining a constant number of genets.

Our simulations suggest that population increases of *A. palmata* may give false hope if those colonies are primarily ramets (Baums et al., 2006). In general, a population dominated by genetically identical individuals is less likely to persist and recover from stress events than diverse populations. Our simulation models also showed that some *Acropora* species may be easier to predict than others. All simulations of corymbose *Acropora* at Aka Jima, largely independent of the year that was used to parameterize the model, accurately predicted the size-frequency distributions through time. These predictions were most likely accurate because there was less variability in the model parameters among years, and fragmentation rates were lower in this species group compared with *A. palmata*. Our results also suggest that the size-frequency distributions of corymbose *Acropora* are not overly useful at determining the occurrence of subtle thermal-stress events in the Pacific through back-propagation analysis, but are probably more useful at determining the occurrence of extreme thermal-stress events (Done et al., 2010; van Woesik et al., 2011). By contrast, simulations of *A. palmata* at Haulover Bay showed that size-frequency distributions were not easy to predict because of the high inter-annual variance in fragmentation rates. Our model showed that thermal-stress events have different effects on two *Acropora* populations, and those events may also be long-lasting. Still, a comparison between only two species, one from the Caribbean and one from the Pacific, does not constitute a representative study of the *Acropora*

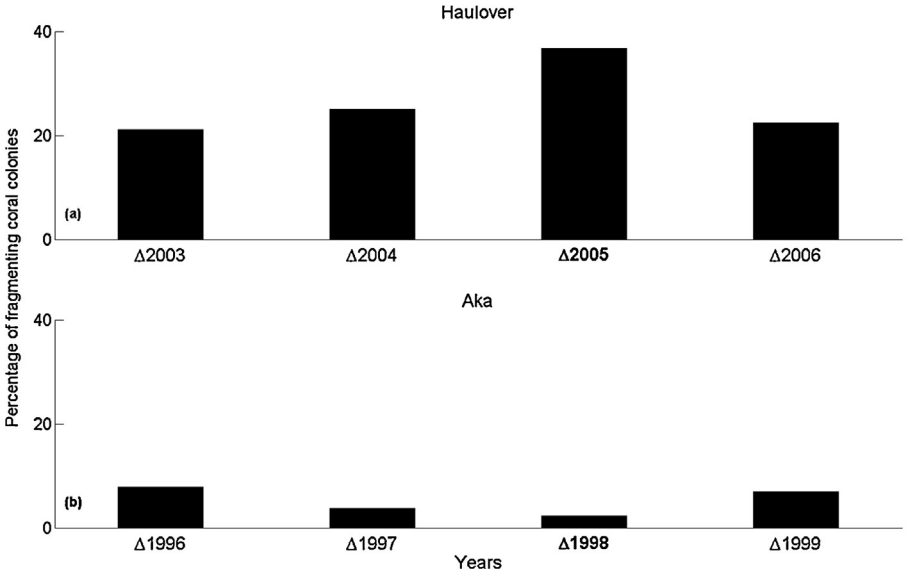

Fig. 3. (a and b) The percentage of coral colonies that fragmented in the field out of the total number of colonies present during four yearly transitions for: (a) Haulover Bay, US Virgin Islands, depicting *Acropora palmata* and (b) Aka Jima, Japan, depicting corymbose *Acropora* (mostly *A. nasuta*). Transitional data are indicated by the delta symbol (Δ) which represents a change from the listed year to the following year (i.e. Δ2003 represents the transition from 2003 to 2004). Bold font indicates the 2005 thermal anomaly in Haulover Bay and the 1998 thermal anomaly in Aka Jima.

response to thermal-stress anomalies. Indeed, it has been recently shown that even among the more temperature-sensitive species, such as *Acropora*, there are winners and losers in rapidly warming oceans (van Woesik et al., 2011).

In summary, this study outlines a novel technique that separates the process of coral-colony fragmentation from colony growth, and tracks the relative contribution of genets and ramets to population dynamics. Differentiating these processes will lead to more accurate predictions of population trajectories through time. Our model showed that the number of *A. palmata* colonies at Haulover Bay have the potential to substantially increase within the next 10 years, although the population will most likely consist of genetically similar individuals, creating a population that may be highly vulnerable to future thermal-stress events. By contrast, corymbose *Acropora* colonies at Aka Jima may be more inclined to undergo directional selection in the warming oceans.

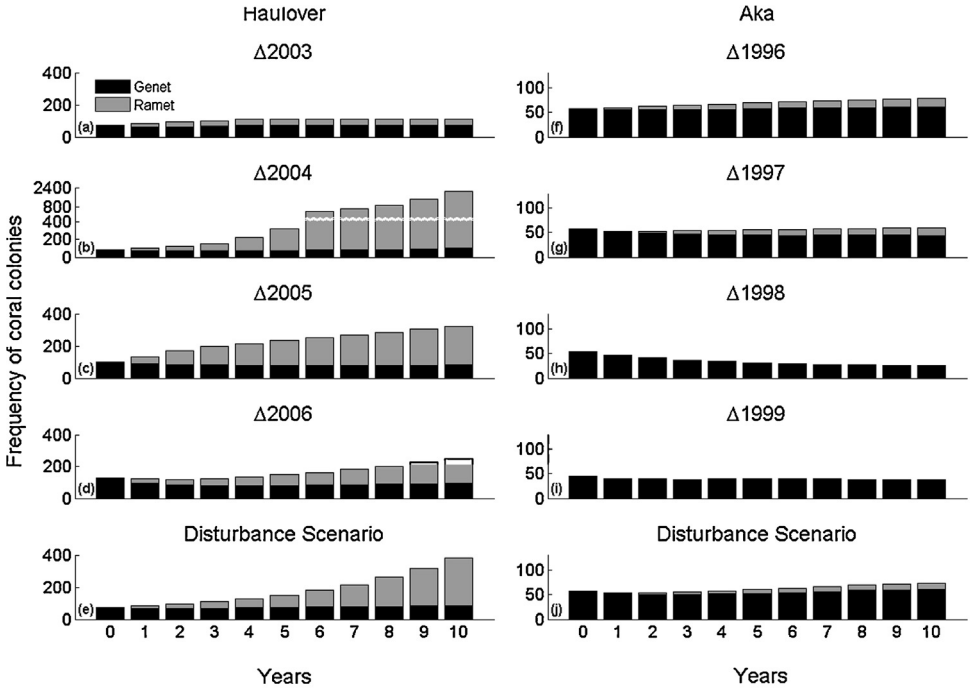

Fig. 4. (a–j) Results using the adjusted Lefkovitch matrix for all data sets from four yearly transitions for Haulover Bay, US Virgin Islands (a–d), and Aka Jima, Japan (f–i), and from the disturbance simulation for Haulover Bay (e), and Aka Jima (j). The disturbance scenario uses an average matrix of all the data matrices (excluding the thermal anomaly years of 2005 for Haulover Bay and 1998 for Aka Jima) for every year except for years 2–3 at both Haulover Bay and Aka Jima. The genet and ramet data for years 2–3 comes from the matrices for the thermal anomalies in 2005 at Haulover Bay, and in 1998 at Aka Jima (Tables 1 and 2). Transitional data are indicated by the delta symbol (Δ) which represents a change from the listed year to the following year (i.e. Δ2003 represents the transition from 2003 to 2004).

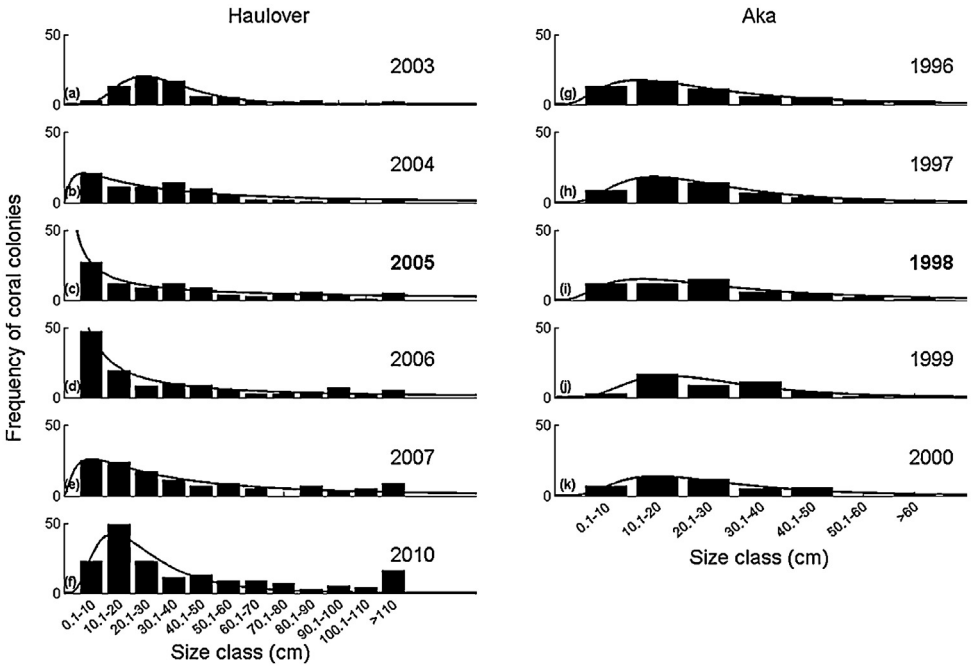

Fig. 5. (a–k) The size-frequency of field data for Haulover Bay, US Virgin Islands, using 12 size classes (a–f), and Aka Jima, Japan, using 7 size classes (g–k). Each size class ranges 10 cm. The abundances are for the entire 500 m × 40 m area in Haulover Bay and the quadrat area of 2 m × 2 m in Aka Jima. Bold font indicates the 2005 thermal anomaly in Haulover Bay (c) and the 1998 thermal anomaly in Aka Jima (i).

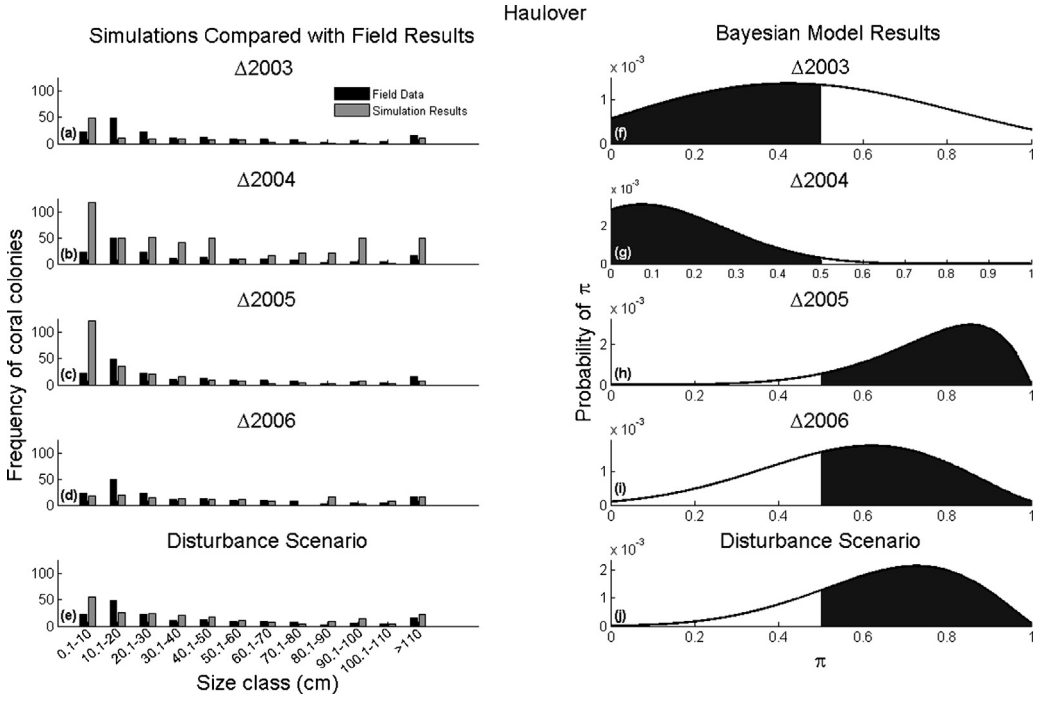

Fig. 6. (a–j) Haulover Bay, US Virgin Islands, size-frequency distributions of field data compared with simulations. The indicated years represent the field data used for each simulation in (a–d). The disturbance scenario is depicted in (e). The disturbance scenario uses an average matrix of all the data matrices (excluding the thermal anomaly year of 2005) for every year except for years 2–3. The data for years 2–3 comes from the matrices for the thermal anomaly in 2005 at Haulover Bay (Table 1). All simulations were run until year 2010 to determine size class abundances for comparison with field data for that year. The Bayesian outputs (f–j) indicate which model type best describes the two distributions (where $\pi > 0.5$ is "over-lapping distribution model" and $\pi < 0.5$ is "distinct distributions model"). The maximum π values for each simulation are (f) 0.423, (g) 0.075, (h) 0.856, (i) 0.621, (j) 0.728. Transitional data are indicated by the delta symbol (Δ) which represents a change from the listed year to the following year (i.e. Δ2003 represents the transition from 2003 to 2004).

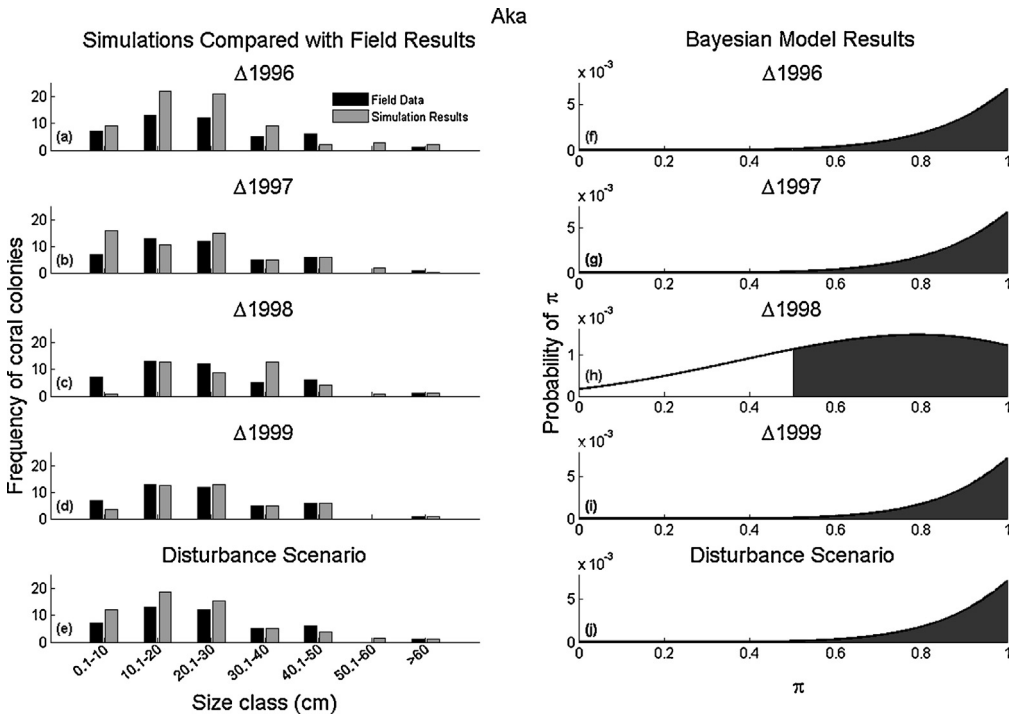

Fig. 7. (a–j) Aka Jima, Japan, size-frequency distributions of field data compared with simulations. The indicated years represent the field data used for each simulation in (a–d). The disturbance scenario is depicted in (e). The disturbance scenario uses an average matrix of all the data matrices (excluding the thermal anomaly year of 1998) for every year except for years 2–3. The data for years 2–3 comes from the matrices for the thermal anomaly in 1998 at Aka Jima (Table 2). All simulations were run until year 2000 to determine size class abundances for comparison with field data for that year. The Bayesian outputs (f–j) indicate which model type best describes the two distributions (where $\pi > 0.5$ is "over-lapping distribution model" and $\pi < 0.5$ is "distinct distributions model"). The maximum π values for each simulation are (f) 1, (g) 1, (h) 0.79, (i) 1, (j) 1. Transitional data are indicated by the delta symbol (Δ) which represents a change from the listed year to the following year (i.e. Δ2003 represents the transition from 2003 to 2004).

Acknowledgments

We would like to thank Jacob Roth for assistance with programming and mathematical interpretations, and Sandra van Woesik for editorial assistance. We would also like to acknowledge those who helped to collect the USVI data including T. Spitzack, A. Bright, R. Brewer, J. Herlan and C.S. Rogers. We would also like to thank the US Geological Survey and C.S. Rogers for providing the data on *Acropora palmata*. E.M.M. was supported by a NOAA Dr. Nancy Foster Scholarship and a Mote Postdoctoral Fellowship.

References

Bak, R.P.M., Steward-van Es, Y., 1980. Regeneration of superficial damage in the scleractinian corals *Agaricia agaricites*, *F. Purpurea* and *Porites astreoides*. Bulletin of Marine Science 30, 883–887.

Baums, I.B., Colin, R.H., Hellberg, M.E., 2005. Mendelian microsatellite loci for the Caribbean coral *Acropora palmata*. Marine Ecology Progress Series 288, 115–127.

Baums, I.B., Miller, M.W., Hellberg, M.E., 2006. Geographic variation in clonal structure in a reef-building Caribbean coral, *Acropora palmata*. Ecological Monographs 76, 503–519.

Betancourt, M., 2010. A Bayesian Approach to Histogram Comparison., pp. 1–19 arXiv:1009.5604v1[hep-th].

Brown, B.E., 1997. Coral bleaching: causes and consequences. Coral Reefs 16, S129–S138.

Done, T.J., 1987. Simulation of the effects of *Acanthaster planci* on the population structure of massive corals in the genus *Porites:* evidence of population resilience? Coral Reefs 6, 75–90.

Done, T., DeVantier, L.M., Turak, E., Fisk, D.A., Wakeford, M., van Woesik, R., 2010. Coral growth on three reefs: development of recovery benchmarks using a space for time approach. Coral Reefs 29, 815–833.

Eakin, C.M., Morgan, J.A., Heron, S.F., Smith, T.B., Liu, G., et al., 2010. Caribbean corals in crisis: record thermal stress, bleaching, and mortality in 2005. PLoS ONE 5 (11), e13969, http://dx.doi.org/10.1371/journal.pone.0013969.

Ellstrand, N.C., Elam, D.R., 1993. Population genetic consequences of small population size: implications for plant conservation. Annual Review of Ecology, Evolution and Systematics 24, 217–242.

Glynn, P.W., 1997. Bioerosion and coral-reef growth: a dynamic balance. In: Birkeland, C. (Ed.), Life and Death of Coral Reefs. Chapman and Hall, New York, pp. 68–95.

Graham, J., van Woesik, R., 2013. The effects of partial mortality on the fecundity of three common Caribbean corals. Marine Biology, http://dx.doi.org/10.1007/s00227-013-2248-y.

Heyward, A.J., Collins, J.D., 1985. Fragmentation in *Montipora ramosa:* the genet and ramet concept applied to a reef coral. Coral Reefs 4, 35–40.

Highsmith, R.C., 1982. Reproduction by fragmentation in corals. Marine Ecology Progress Series 7, 207–226.

Highsmith, R.C., Riggs, A.C., D'Antonio, C.M., 1980. Survival of hurricane-generated coral fragments and a disturbance model of reef calcification/growth rates. Oecologia 46, 322–329.

Hoegh-Guldberg, O., 1999. Climate change coral bleaching and the future of the world's coral reefs. Marine Freshwater Research 50, 839–866.

Hughes, T.P., 1984. Population dynamics based on individual size rather than age: a general model with a reef coral example. American Naturalist 123, 778–795.

Jackson, J.B.C., 1977. Competition of marine hard substrata: the adaptive significance of solitary and colonies strategies. American Naturalist 111, 743–767.

Lefkovitch, L.P., 1965. The study of population growth in organisms grouped by stages. Biometrics 21, 1–18.

Lesser, M.P., 1996. Oxidative stress causes coral bleaching during exposure to elevated temperatures. Coral Reefs 16, 187–192.

Lirman, D., 2000. Fragmentation in the branching coral *Acropora palmata* (Lamarck): growth, survivorship, and reproduction of colonies and fragments. Journal of Experimental Marine Biology and Ecology 251, 41–57.

Loya, Y., Sakai, K., Yamazato, K., Nakano, Y., Sambali, H., van Woesik, R., 2001. Coral bleaching: the winners and the losers. Ecology Letters 4, 122–131.

Meesters, E.H., Bak, R.P.M., 1993. Effects of coral bleaching on tissue regeneration potential and colony survivial. Marine Ecology Progress Series 96, 189–198.

Muller, E.M., Rogers, C.S., Spitzack, A., van Woesik, R., 2008. Bleaching increases the likelihood of disease on *Acropora palmata* (Lamarck) at Hawksnest Bay, St. John, US Virgin Islands. Coral Reefs 27, 191–195.

Orive, M.A., 1995. Senescence in organisms with clonal reproduction and complex life histories. American Naturalist 145, 90–108.

Rogers, C.S., Muller, E.M., 2012. Bleaching disease and recovery in the threatened scleractinian coral *Acropora palmata* in St. John, US Virgin Islands: 2003–2010. Coral Reefs 31, 807–818.

Roth, L., Koksal, S., van Woesik, R., 2010. Effects of thermal stress on key processes driving coral-population dynamics. Marine Ecology Progress Series 411, 73–87.

Stimson, J., Sakai, K., Sembali, H., 2002. Interspecific comparison of the symbiotic relationship in corals with high and low rates of bleaching-induced mortality. Coral Reefs 21, 409–421.
van Woesik, R., Jordan-Garza, A.G., 2011. Coral populations in a rapidly changing environment. Journal of Experimental Marine Biology and Ecology 408, 11–20.
van Woesik, R., Sakai, K., Ganase, A., Loya, Y., 2011. Revisiting the winners and loser a decade after coral bleaching. Marine Ecology Progress Series 434, 67–76.
Worm, B., Barbier, E.B., Beaumont, N., Duffy, J.E., Folke, C., Halpern, B.S., Jackson, J.B., Lotze, H.K., Micheli, F., Palumbi, S.R., Sala, E., Selkoe, K.A., Stachowicz, Watson, R., 2006. Impacts of biodiversity loss on ocean ecosystem services. Science 314, 787–790.